

# Single-Cell RNA-seq Analysis Report

## Spatiotemporal Dynamics of Myocardial Remodeling in Mouse TAC Model

OmicsDesk

2026-04-03

### Table of contents

<b>1</b>	<b>Executive Summary</b>	<b>3</b>
<b>2</b>	<b>Methods</b>	<b>4</b>
2.1	Quality Control & Preprocessing . . . . .	4
2.2	Normalization & Dimensionality Reduction . . . . .	4
2.3	Batch Integration . . . . .	4
2.4	Clustering . . . . .	4
2.5	Cell Type Annotation . . . . .	4
2.6	Marker Genes & Differential Expression . . . . .	4
2.7	Spatial Integration . . . . .	4
<b>3</b>	<b>Quality Control</b>	<b>5</b>
3.1	QC Summary . . . . .	5
3.2	QC Distributions (Pre-filter) . . . . .	5
3.3	QC Distributions (Post-filter) . . . . .	5
3.4	QC Metrics per Sample . . . . .	6
3.5	PCA Variance . . . . .	6
<b>4</b>	<b>Clustering &amp; Cell Types</b>	<b>7</b>
4.1	Dataset Overview . . . . .	7
4.2	Cell Types . . . . .	7
4.3	Cell Type Composition . . . . .	7
4.4	Composition per Cluster . . . . .	8
4.5	Cell Type Proportions per Sample . . . . .	9
<b>5</b>	<b>Marker Genes</b>	<b>10</b>
5.1	Dot Plot — Top Markers per Cluster . . . . .	10
5.2	Heatmap — Top Markers . . . . .	10
5.3	Marker Violin Plots . . . . .	11
5.4	Top Marker Genes . . . . .	11
<b>6</b>	<b>Differential Expression</b>	<b>14</b>
6.1	Results Summary . . . . .	14
6.2	Volcano Plots . . . . .	14
6.3	Top Differentially Expressed Genes (Up-regulated) . . . . .	17
6.4	Top Differentially Expressed Genes (Down-regulated) . . . . .	17
6.5	Cell Type Distribution per Condition . . . . .	17
<b>7</b>	<b>Differential Abundance</b>	<b>18</b>

<b>8 Trajectory Analysis</b>	<b>19</b>
<b>9 Spatial Analysis</b>	<b>21</b>
9.1 Spatially Variable Genes (Moran's I) . . . . .	21
9.2 Cell Type Spatial Mapping . . . . .	22
9.3 Differential Expression — Spatial Overlay . . . . .	23
9.4 Cell Type Co-localization . . . . .	24
<b>10 Conclusions</b>	<b>25</b>

## 1 Executive Summary

This report presents a single-cell RNA sequencing (scRNA-seq) analysis of myocardial remodeling in a mouse transverse aortic constriction (TAC) model across four conditions: Sham control, and TAC at 2, 4, and 6 weeks post-surgery. After quality filtering, 27,146 high-quality cells were retained across all four samples. **Cell type landscape.** Marker-based annotation identified eight major cell populations. The cardiac microenvironment is dominated by fibroblasts (41.1%), consistent with the pronounced fibrotic remodeling expected in pressure-overload models. Macrophages represent the second largest population (20.3%), reflecting an active inflammatory response. B cells (14.2%) and neutrophils (9.0%) indicate sustained immune infiltration. Endothelial cells (7.3%), T cells (5.6%), cardiomyocytes (1.4%), and smooth muscle cells (1.1%) complete the cellular landscape. The low cardiomyocyte capture rate is expected in droplet-based scRNA-seq due to their large cell size. **Temporal dynamics.** Cell type composition shifts markedly over the TAC time course. At 4 and 6 weeks, B cell and macrophage proportions increase substantially compared to Sham, while fibroblast proportions decrease relatively — suggesting a progressive transition from a fibrosis-dominated to an inflammation-dominated microenvironment as heart failure advances. **Differential expression.** At 2 weeks post-TAC, the transcriptomic response is modest (12 upregulated, 8 downregulated genes;  $\text{padj} < 0.05$ ,  $|\log_2\text{FC}| > 1$ ). The top upregulated gene is *Nppa* (atrial natriuretic peptide), a canonical marker of cardiac stress and heart failure. By 6 weeks, the response is dramatically amplified: 73 genes are upregulated and 697 are downregulated. Upregulated genes are enriched for ribosomal proteins (*Rps28*, *Rpl36*, *Rpl37*, *Rpl38*), indicating increased translational activity, and B cell markers (*Igkc*, *Cd79a*), confirming the immune cell infiltration observed in the composition analysis. Downregulated genes include hemoglobin subunits (*Hbb-bs*, *Hba-a1*, *Hba-a2*;  $\log_2\text{FC} = -3.7$  to  $-4.6$ ) and multiple mitochondrial genes (*mt-Nd5*, *mt-Nd2*, *mt-Nd4*, *mt-Cytb*, *mt-Atf6*), pointing to mitochondrial dysfunction — a hallmark of the failing heart. Additionally, *Vim* (vimentin) and *Rock1* (Rho-kinase, involved in cardiac fibrosis signaling) are significantly downregulated at 6 weeks.

## 2 Methods

### 2.1 Quality Control & Preprocessing

Raw count matrices (10x Genomics Cell Ranger output) were loaded using **scanpy** (v1.9+). Per-cell quality metrics were computed: number of detected genes, total UMI counts, and percentage of mitochondrial reads (mt- prefix). Doublets were detected and removed using **Scrublet** (v0.2+) with default parameters. Cells were filtered to retain those with:

- Genes per cell: see QC table
- Maximum mitochondrial fraction: see QC table

### 2.2 Normalization & Dimensionality Reduction

Library-size normalization was applied (**scanpy** `normalize_total`, target sum = 10,000), followed by log1p transformation. Highly variable genes (HVGs) were selected using the Seurat v3 method (top 2,000 genes). Data were scaled (max value = 10) and principal component analysis (PCA) was performed on HVGs (50 components).

### 2.3 Batch Integration

When multiple samples were present, batch effects were corrected using **Harmony** (`harmonypy`) on PCA embeddings, with sample identity as the batch key.

### 2.4 Clustering

A k-nearest neighbors graph was constructed (k = 15, 30 PCs) and cells were embedded using **UMAP**. Community detection was performed using the **Leiden** algorithm (igraph implementation).

### 2.5 Cell Type Annotation

Automated cell type annotation was performed using **CellTypist** with majority voting to assign consensus labels per Leiden cluster. The model was selected based on organism (mouse).

### 2.6 Marker Genes & Differential Expression

Cluster marker genes were identified using the Wilcoxon rank-sum test (**scanpy** `rank_genes_groups`, `groupby = leiden`). For condition-based differential expression, the same test was applied per contrast (numerator vs. denominator conditions). Significance thresholds: adjusted p-value (Benjamini-Hochberg) < 0.05,  $|\log_2 \text{fold-change}| > 1$ .

### 2.7 Spatial Integration

Spatial transcriptomics data (10x Visium) were processed with **squidpy** (v1.2+). A spatial neighborhood graph was constructed (generic coordinates, k = 10 neighbors). Spatially variable genes were identified using **Moran's I** autocorrelation statistic on the top 100 HVGs. Cell type labels were transferred from the scRNA-seq reference by scoring each spatial spot for marker gene enrichment (**scanpy** `tl.score_genes`) using the top 15 marker genes per cell type, and assigning the cell type with the highest score. Neighborhood enrichment analysis was performed using the transferred cell type labels to assess spatial co-localization patterns.

### 3 Quality Control

#### 3.1 QC Summary

Table 1: Per-sample QC metrics after filtering.

Sample	Cells (post-filter)	Median genes/cell	Median UMIs/cell	Median % mito
Sham	8218	2634	8931	4.5
TAC2w	6577	2911	10379	4.6
TAC4w	6811	1390	4356	5.0
TAC6w	5540	1639	4673	2.6

#### 3.2 QC Distributions (Pre-filter)

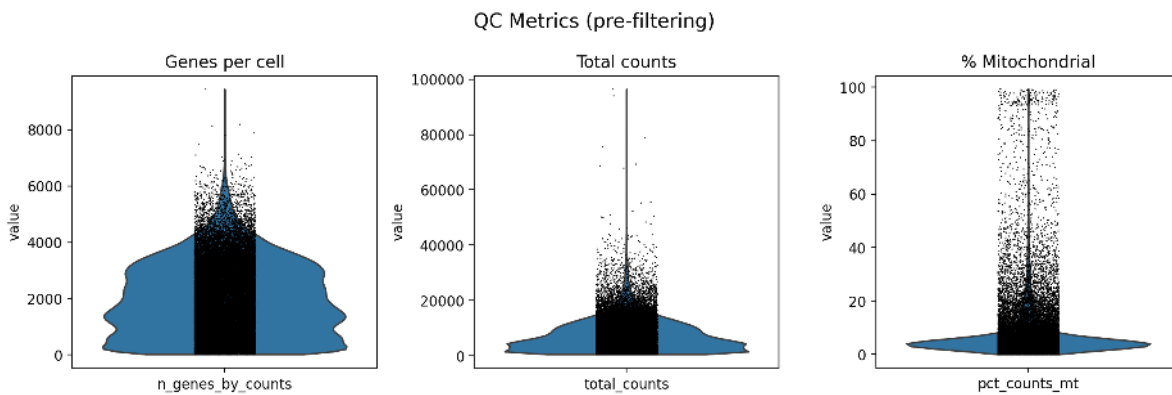


Figure 1: QC metrics before filtering: genes per cell, total UMI counts, and percentage mitochondrial reads.

#### 3.3 QC Distributions (Post-filter)

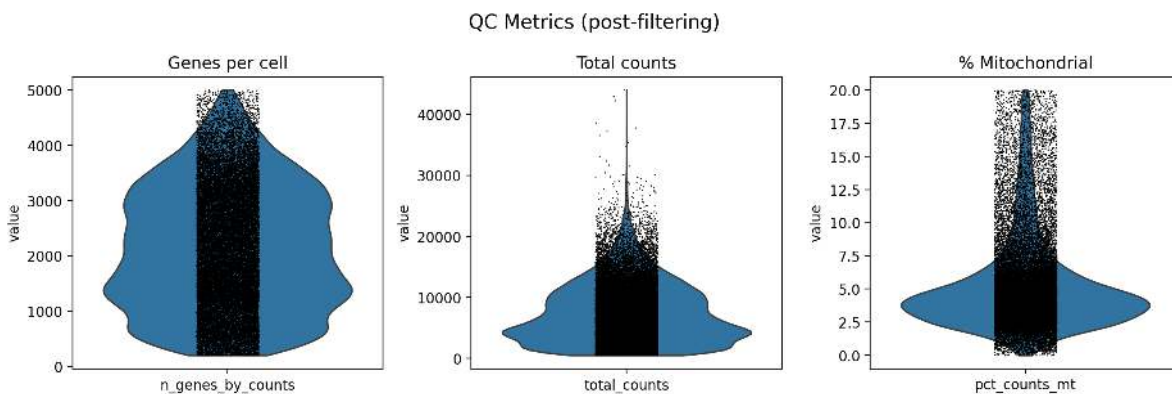


Figure 2: QC metrics after filtering and doublet removal.

### 3.4 QC Metrics per Sample

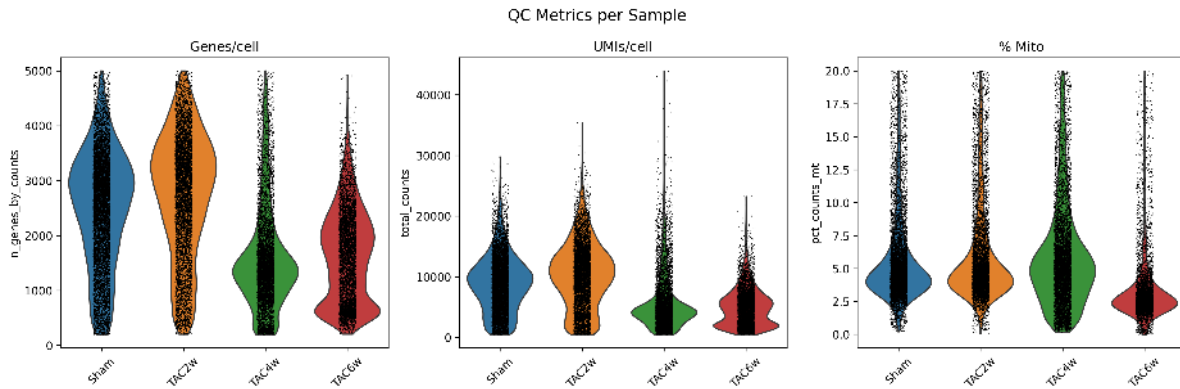


Figure 3: Distribution of genes per cell, UMIs per cell, and mitochondrial fraction across samples.

### 3.5 PCA Variance

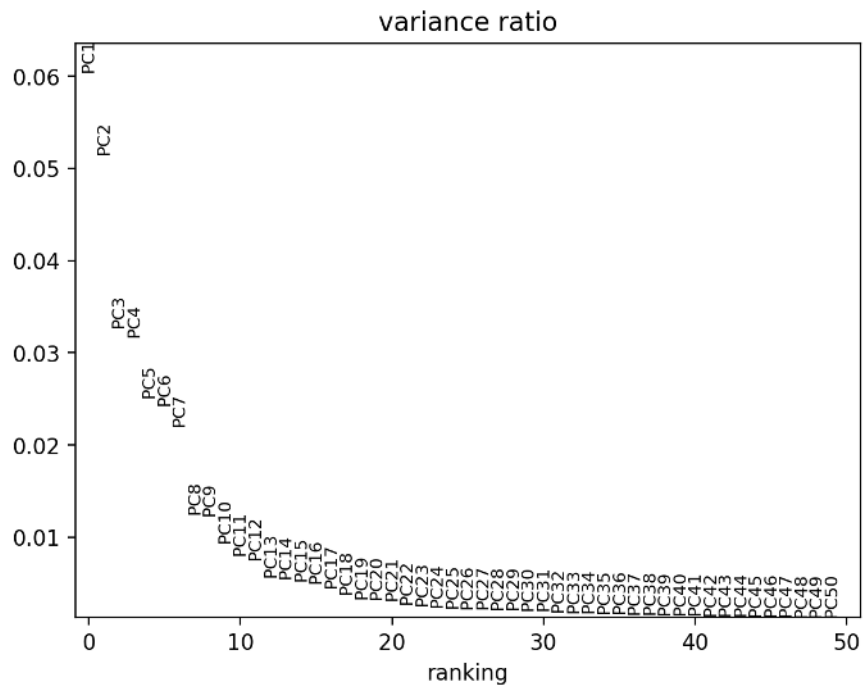


Figure 4: Proportion of variance explained by each principal component.

## 4 Clustering & Cell Types

### 4.1 Dataset Overview

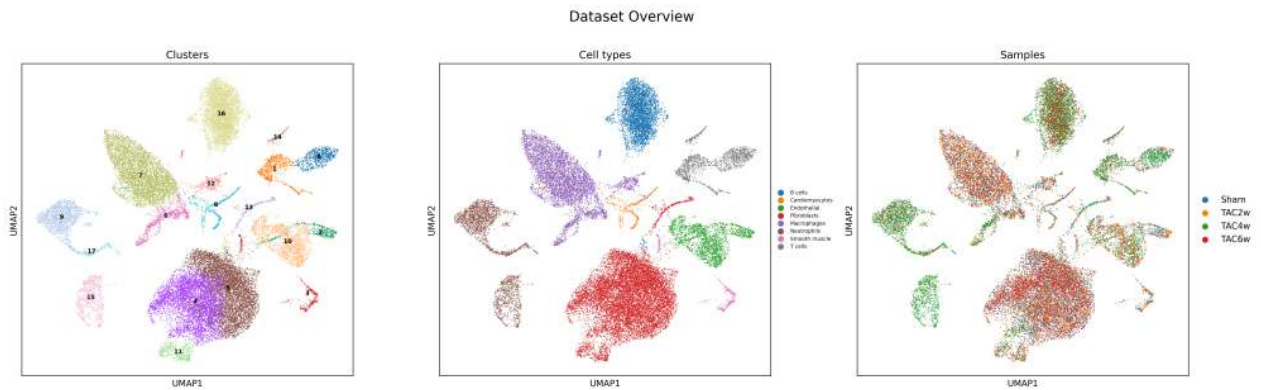


Figure 5: UMAP projections colored by Leiden cluster, cell type annotation, and sample of origin.

### 4.2 Cell Types

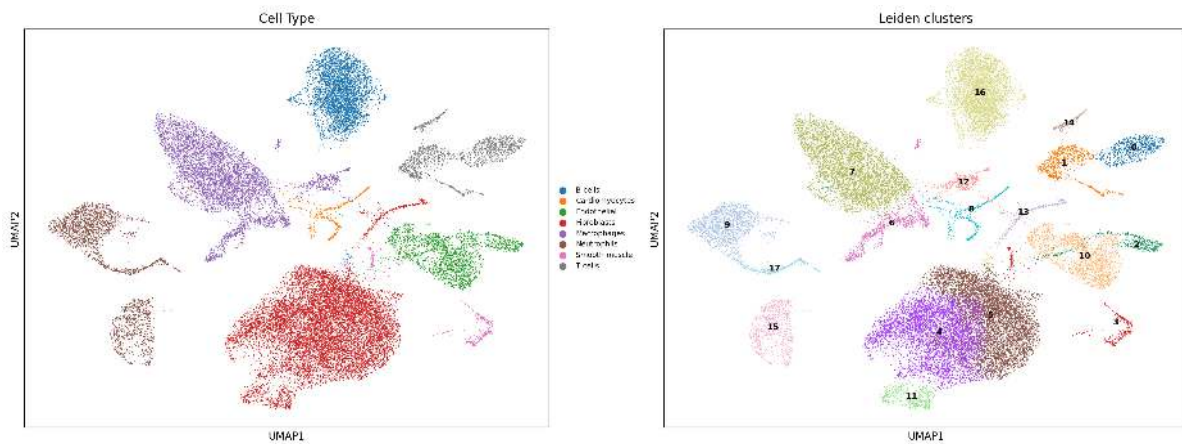


Figure 6: UMAP colored by CellTypist annotation (majority voting) alongside Leiden clusters.

### 4.3 Cell Type Composition

Table 2: Cell type counts and proportions.

Cell Type	Count	Percentage
Fibroblasts	11170	41.1
Macrophages	5515	20.3
B cells	3855	14.2
Neutrophils	2439	9.0
Endothelial	1983	7.3
T cells	1517	5.6
Cardiomyocytes	378	1.4
Smooth muscle	289	1.1

## 4.4 Composition per Cluster

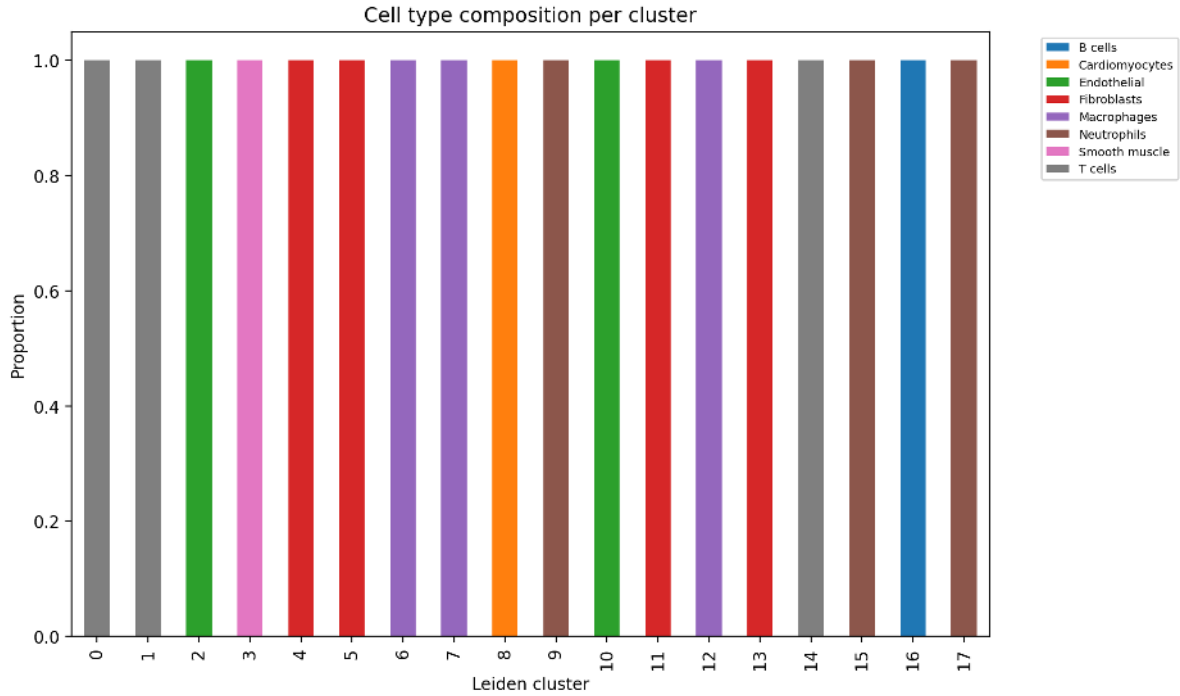


Figure 7: Cell type composition within each Leiden cluster.

## 4.5 Cell Type Proportions per Sample

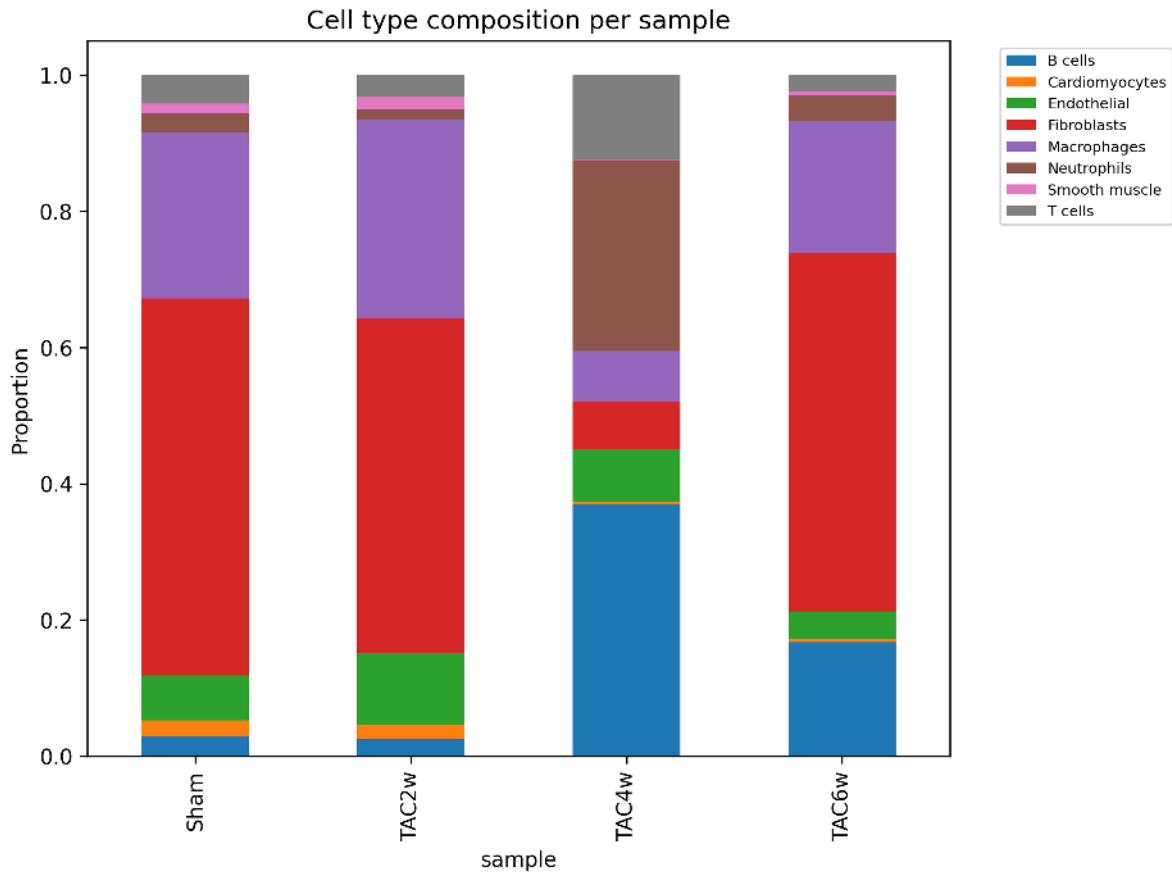


Figure 8: Stacked bar chart of cell type proportions across samples/conditions.



### 5.3 Marker Violin Plots

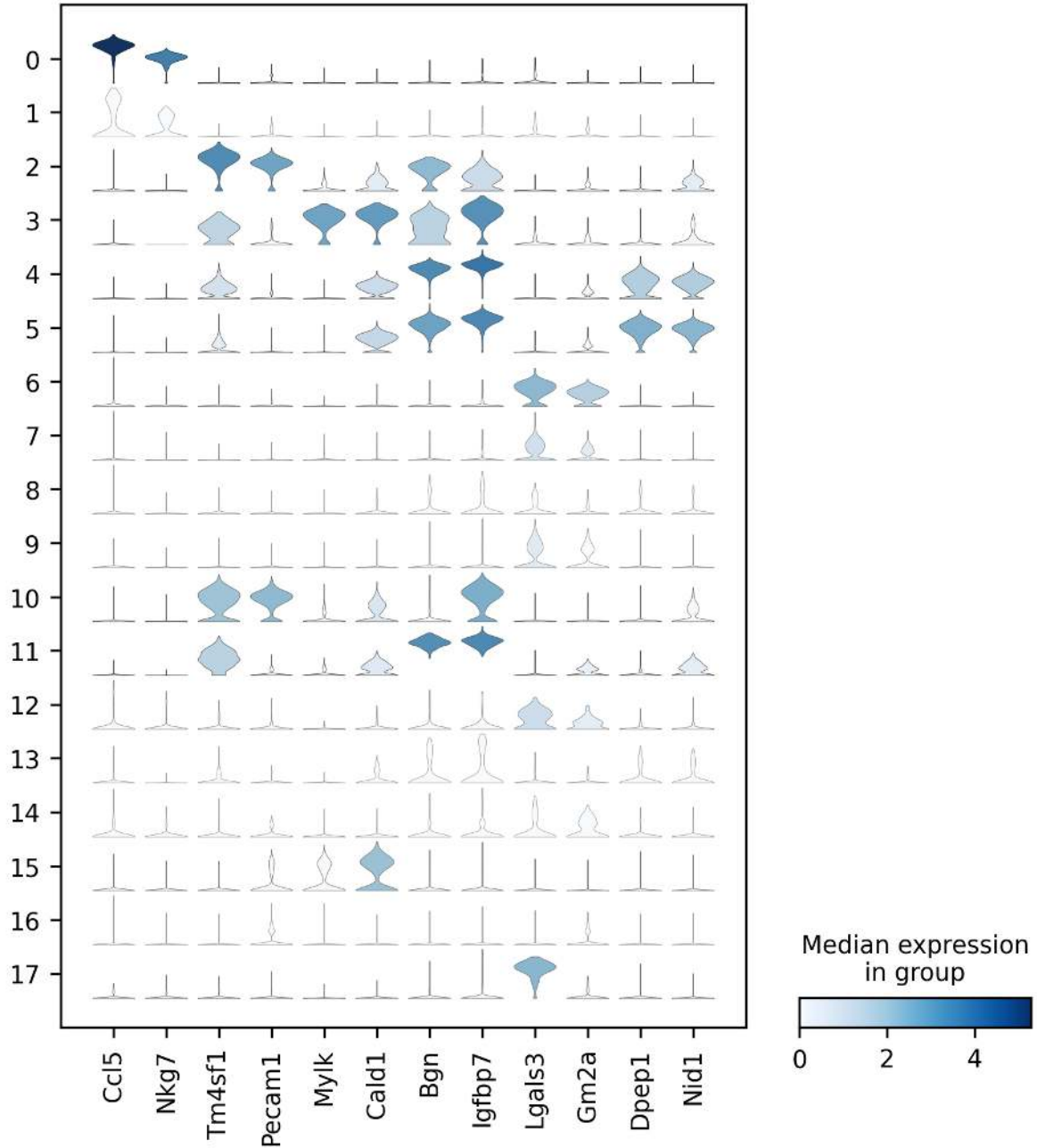


Figure 11: Stacked violin plot of top marker genes across Leiden clusters.

### 5.4 Top Marker Genes

Table 3: Top 5 marker genes per cluster (Wilcoxon rank-sum test, ordered by score).

Cluster	Gene	Score	log2FC	padj
0	Ccl5	42.91	10.60	0
0	Nkg7	42.77	9.39	0
0	AW112010	41.97	6.63	0
0	Klrk1	41.48	8.26	0
0	Klre1	41.23	10.12	0
1	Trbc2	40.59	8.01	0
1	Cd3g	38.28	8.28	0
1	Cd3d	37.75	8.14	0
1	Lck	35.17	6.27	0
1	Ets1	34.58	3.45	0
2	Tm4sf1	29.75	5.09	0
2	Pecam1	29.75	5.37	0
2	Emcn	29.64	6.56	0
2	Eng	28.70	4.57	0
2	Cavin2	28.35	4.83	0
3	Mylk	25.38	7.08	0
3	Cald1	25.18	4.12	0
3	Mfge8	24.68	3.94	0
3	Gucy1a1	23.89	5.65	0
3	Tpm2	23.71	7.11	0
4	Bgn	91.42	4.17	0
4	Igfbp7	90.69	4.20	0
4	Serpinf1	88.33	3.51	0
4	Pmepa1	86.78	3.37	0
4	Mfap5	86.65	4.10	0
5	Dpep1	94.82	4.27	0
5	Nid1	94.45	3.76	0
5	Serping1	92.37	4.00	0
5	Tnxb	91.44	3.61	0
5	Gpx3	90.71	3.82	0
6	Lgals3	35.36	4.11	0
6	Gm2a	32.73	2.98	0
6	Napsa	32.36	3.61	0
6	Gpx1	31.98	2.21	0
6	Ctss	30.94	3.09	0
7	C1qa	101.56	8.15	0
7	C1qb	101.50	7.99	0
7	C1qc	100.52	7.88	0
7	Lyz2	96.32	6.41	0
7	Csf1r	95.34	5.95	0
8	Tnni3	32.50	8.40	0
8	Tnnt2	32.50	8.33	0
8	Tpm1	31.94	6.52	0
8	Mb	31.71	8.24	0
8	Tnnc1	30.55	8.38	0
9	Il1r2	63.06	9.19	0
9	Srgn	62.52	5.57	0
9	Cebpb	62.41	4.97	0
9	Msrb1	62.36	6.49	0
9	Il1b	62.27	8.60	0
10	Fabp4	66.14	8.57	0
10	Cd36	61.41	7.02	0
10	Ly6c1	59.59	6.48	0
10	Flt1	59.07	7.50	0
10	Adgrf5	57.40	7.49	0

Table 3: Top 5 marker genes per cluster (Wilcoxon rank-sum test, ordered by score). (*continued*)

Cluster	Gene	Score	log2FC	padj
11	Dkk3	34.43	5.73	0
11	Prelp	33.06	4.52	0
11	Ecrq4	31.37	6.94	0
11	Vim	29.70	2.85	0
11	Il11ra1	29.19	3.15	0
12	Mki67	31.47	8.31	0
12	Hmgb2	30.46	4.45	0
12	Top2a	30.09	8.32	0
12	Tubb5	30.06	3.58	0
12	Stmn1	30.01	6.72	0
13	Hba-a2	27.76	10.91	0
13	Hbb-bs	27.76	10.74	0
13	Hba-a1	27.75	10.79	0
13	Hbb-bt	27.59	10.65	0
13	Alas2	26.89	10.09	0
14	Il7r	19.61	7.63	0
14	Emb	17.52	4.99	0
14	Ccr2	16.28	5.18	0
14	S100a4	16.22	4.49	0
14	Cxcr6	15.79	7.90	0
15	Nrgn	45.88	10.94	0
15	Ctla2a	45.86	9.90	0
15	Gng11	45.84	8.03	0
15	Cd9	45.67	5.99	0
15	Tmsb4x	45.62	4.54	0
16	Cd79a	95.06	9.74	0
16	Ighm	95.02	6.23	0
16	Igkc	94.25	9.67	0
16	Cd79b	89.34	7.77	0
16	Ebf1	87.47	4.02	0
17	S100a9	28.99	11.32	0
17	S100a8	28.98	11.19	0
17	Lcn2	28.98	9.72	0
17	Ngp	28.91	12.07	0
17	Wfdc21	28.89	8.78	0

## 6 Differential Expression

### 6.1 Results Summary

Table 4: DEG counts ( $\text{padj} < 0.05$ ,  $|\log_2\text{FC}| > 1$ )

contrast	Total tested	Sig. UP	Sig. DOWN
TAC2w_vs_Sham	32285	12	8
TAC6w_vs_Sham	32285	73	697

### 6.2 Volcano Plots

#### 6.2.1 12\_volcano\_TAC2w\_vs\_Sham

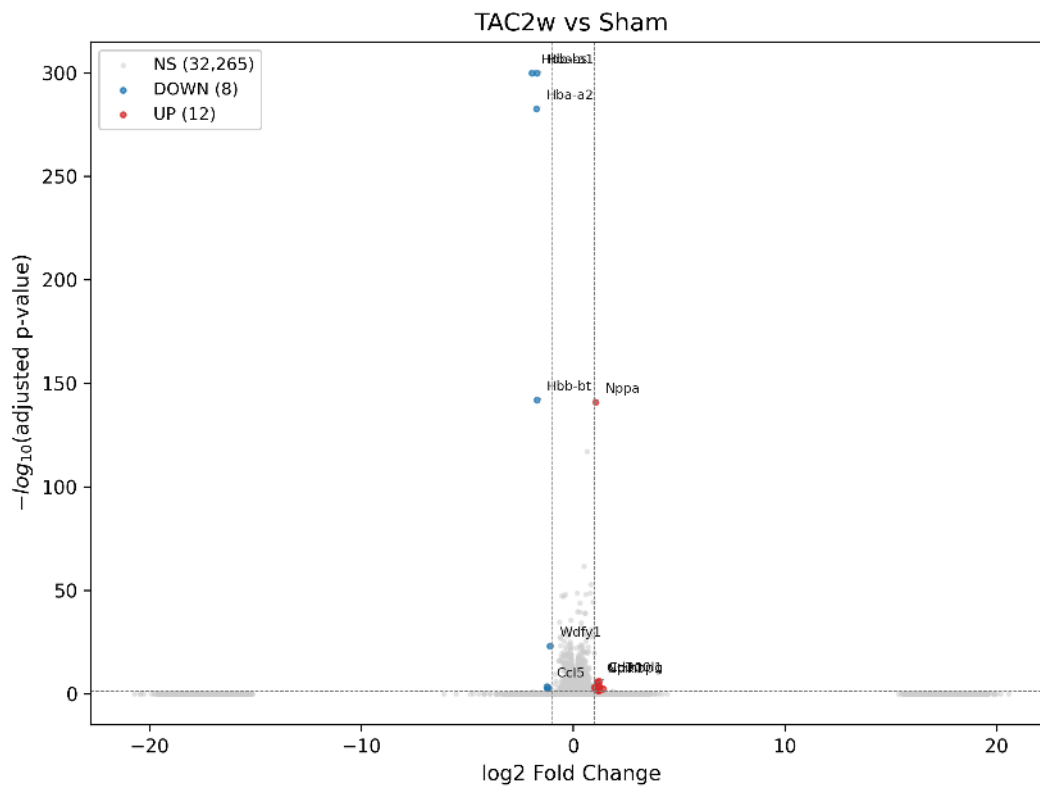


Figure 12: Volcano plot: 12\_volcano\_TAC2w\_vs\_Sham. Crimson: significant; grey: not significant.

### 6.2.2 12\_volcano\_TAC6w\_vs\_Sham

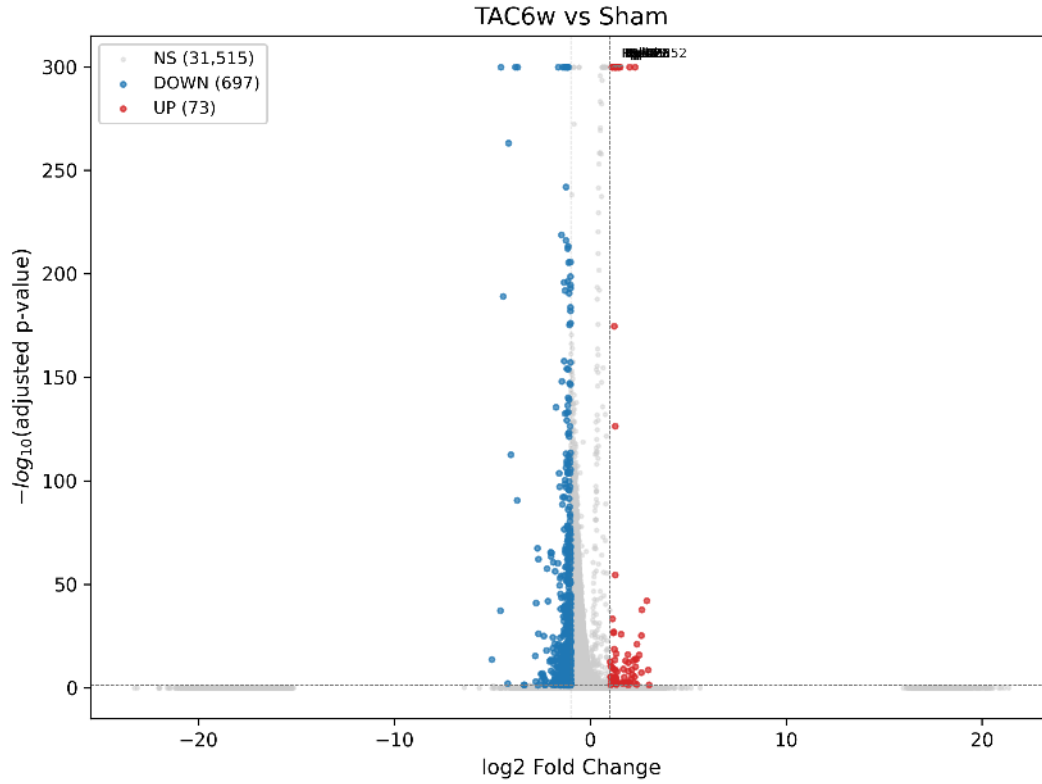


Figure 13: Volcano plot: 12\_volcano\_TAC6w\_vs\_Sham. Crimson: significant; grey: not significant.

Table 5: Top up-regulated genes per contrast (ordered by adjusted p-value).

Contrast	Gene	log2FC	padj
TAC2w_vs_Sham	Nppa	1.06	0.00e+00
TAC2w_vs_Sham	Cd300lg	1.22	1.00e-06
TAC2w_vs_Sham	Gpihbp1	1.13	1.50e-06
TAC2w_vs_Sham	Ntrk1	1.15	4.00e-06
TAC2w_vs_Sham	Timp4	1.25	3.71e-04
TAC2w_vs_Sham	Adgrl4	1.00	5.22e-04
TAC2w_vs_Sham	Rbp7	1.20	5.99e-04
TAC2w_vs_Sham	Gm42031	1.05	2.39e-03
TAC2w_vs_Sham	Btnl9	1.43	6.38e-03
TAC2w_vs_Sham	C1qtnf9	1.24	2.08e-02
TAC2w_vs_Sham	Tcf15	1.16	2.32e-02
TAC2w_vs_Sham	Slc15a2	1.20	4.25e-02
TAC6w_vs_Sham	Rps28	1.53	0.00e+00
TAC6w_vs_Sham	Uba52	2.30	0.00e+00
TAC6w_vs_Sham	Rps29	1.33	0.00e+00
TAC6w_vs_Sham	Rps27	1.44	0.00e+00
TAC6w_vs_Sham	Rpl37a	1.23	0.00e+00
TAC6w_vs_Sham	Rpl35	1.43	0.00e+00
TAC6w_vs_Sham	Rpl37	1.10	0.00e+00
TAC6w_vs_Sham	Rps21	1.22	0.00e+00
TAC6w_vs_Sham	Rpl38	1.28	0.00e+00
TAC6w_vs_Sham	Rpl36	1.11	0.00e+00
TAC6w_vs_Sham	Gm11808	2.02	0.00e+00
TAC6w_vs_Sham	Tmsb10	1.34	0.00e+00
TAC6w_vs_Sham	Btg1	1.23	0.00e+00
TAC6w_vs_Sham	Bloc1s1	1.26	0.00e+00
TAC6w_vs_Sham	Jup	1.27	0.00e+00

Table 6: Top down-regulated genes per contrast (ordered by adjusted p-value).

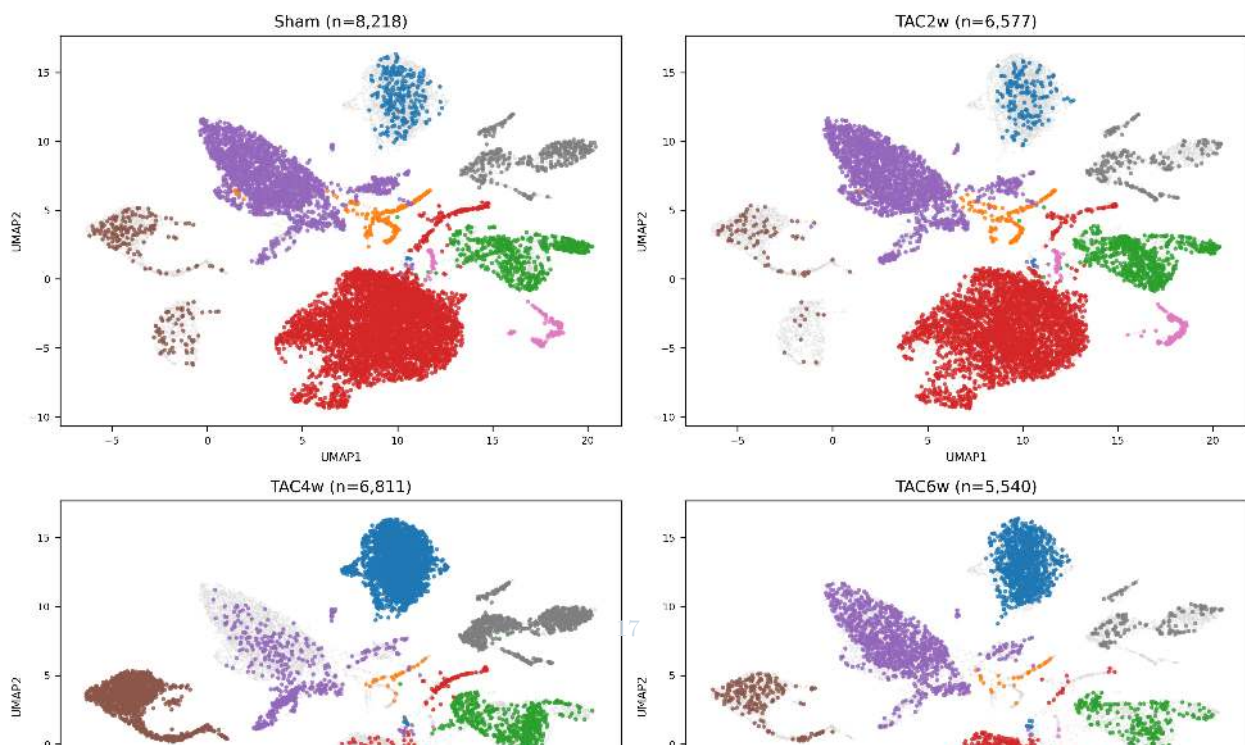
Contrast	Gene	log2FC	padj
TAC2w_vs_Sham	Hba-a1	-1.71	0.000000
TAC2w_vs_Sham	Hbb-bs	-1.95	0.000000
TAC2w_vs_Sham	Hba-a2	-1.73	0.000000
TAC2w_vs_Sham	Hbb-bt	-1.71	0.000000
TAC2w_vs_Sham	Wdfy1	-1.10	0.000000
TAC2w_vs_Sham	Ccl5	-1.23	0.000337
TAC2w_vs_Sham	Cadm3	-1.18	0.001120
TAC2w_vs_Sham	Stmn4	-1.21	0.002690
TAC6w_vs_Sham	mt-Nd5	-1.24	0.000000
TAC6w_vs_Sham	Hba-a2	-3.82	0.000000
TAC6w_vs_Sham	Hba-a1	-3.72	0.000000
TAC6w_vs_Sham	mt-Cytb	-1.16	0.000000
TAC6w_vs_Sham	mt-Nd4	-1.41	0.000000
TAC6w_vs_Sham	mt-Atp6	-1.18	0.000000
TAC6w_vs_Sham	mt-Nd2	-1.64	0.000000
TAC6w_vs_Sham	Hbb-bs	-4.57	0.000000
TAC6w_vs_Sham	Npm1	-1.11	0.000000
TAC6w_vs_Sham	Sept7	-1.31	0.000000
TAC6w_vs_Sham	Hbb-bt	-4.16	0.000000
TAC6w_vs_Sham	Capza2	-1.24	0.000000
TAC6w_vs_Sham	Pid1	-1.48	0.000000
TAC6w_vs_Sham	Atrx	-1.23	0.000000
TAC6w_vs_Sham	Sdcbp	-1.13	0.000000

### 6.3 Top Differentially Expressed Genes (Up-regulated)

### 6.4 Top Differentially Expressed Genes (Down-regulated)

### 6.5 Cell Type Distribution per Condition

Cell Types per Condition



## 7 Differential Abundance

Table 7: Differential abundance testing of cell type proportions across conditions (scCODA).

cell_type	Sham (%)	TAC2w (%)	TAC4w (%)	TAC6w (%)	FDR	Significant
B cells	3.0	2.5	37.0	16.8	0	Yes
Cardiomyocytes	2.3	2.2	0.4	0.5	0	Yes
Endothelial	6.6	10.6	7.7	3.9	0	Yes
Fibroblasts	55.3	49.0	6.9	52.8	0	Yes
Macrophages	24.5	29.3	7.4	19.3	0	Yes
Neutrophils	2.7	1.4	28.1	3.8	0	Yes
Smooth muscle	1.5	1.9	0.2	0.5	0	Yes
T cells	4.1	3.1	12.3	2.4	0	Yes

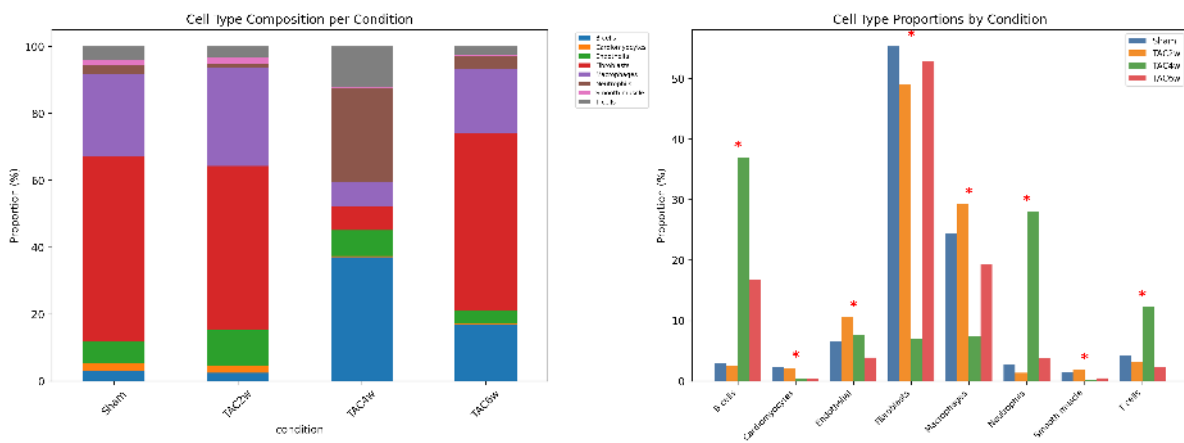


Figure 15: Cell type proportion changes across conditions with statistical significance.

## 8 Trajectory Analysis

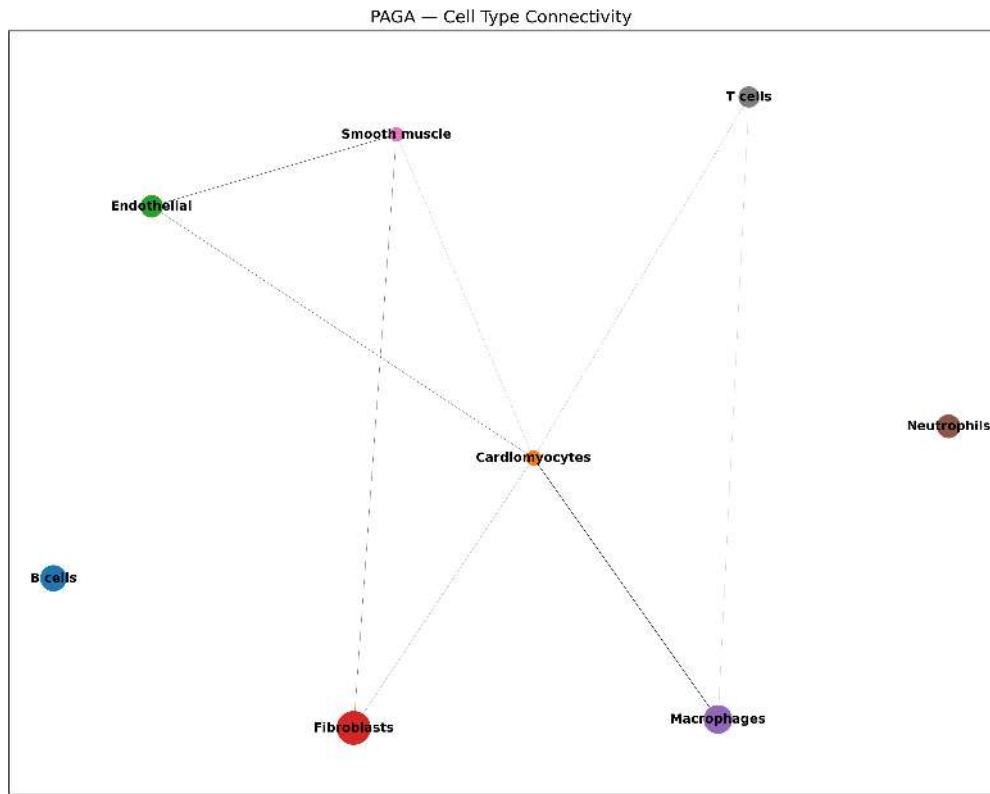


Figure 16: PAGA graph showing connectivity between cell type clusters. Edge thickness indicates connectivity strength.

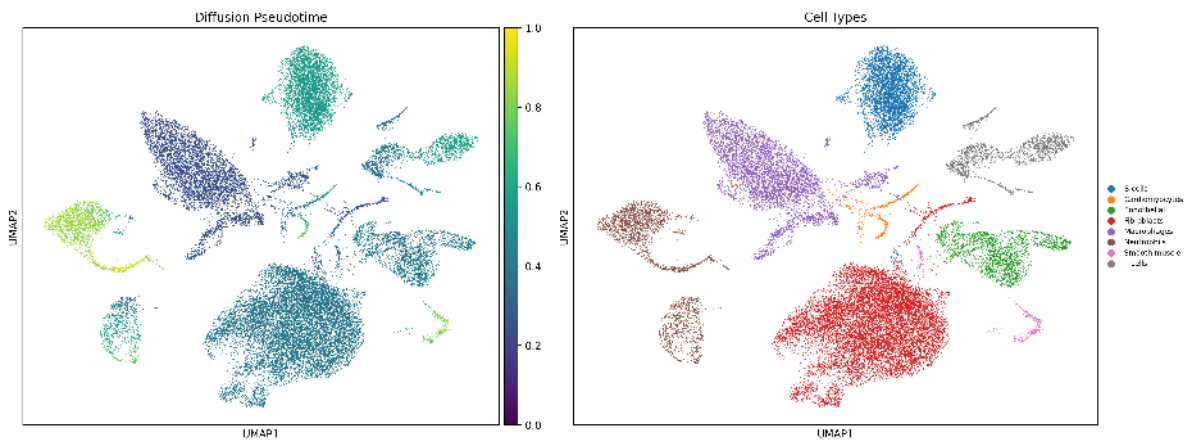


Figure 17: Diffusion pseudotime projected onto UMAP. Color indicates pseudotime progression from root cell.

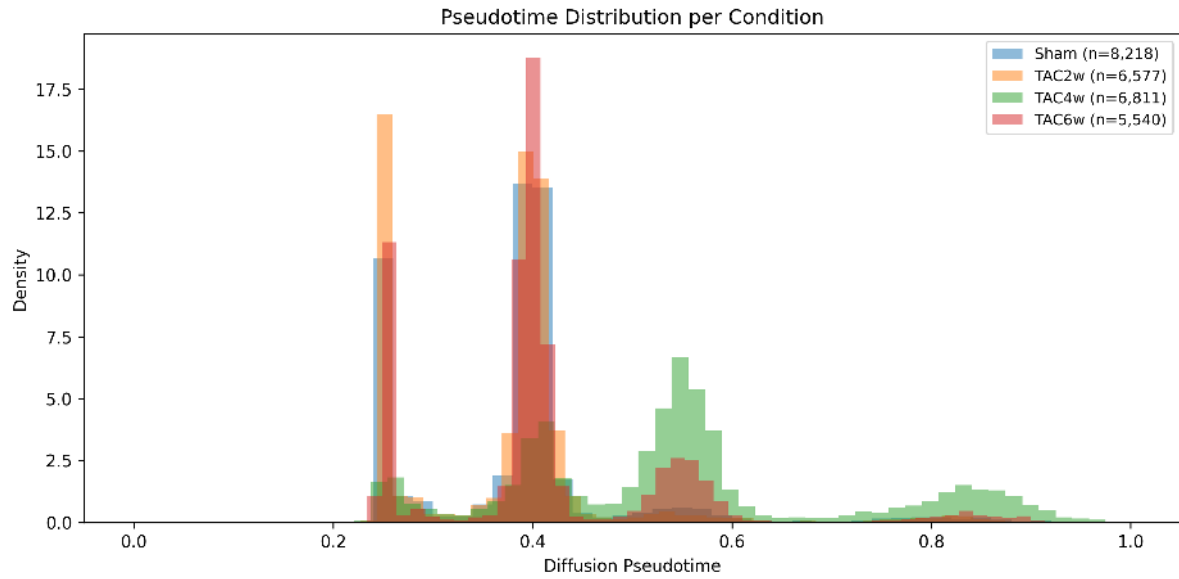


Figure 18: Pseudotime distribution per condition, showing cell state progression across timepoints.

## 9 Spatial Analysis

### 9.1 Spatially Variable Genes (Moran's I)

Table 8: Top 20 spatially variable genes ranked by Moran's I statistic.

...1	I	pval_norm	var_norm	pval_norm	fdr_bh
Ttn	0.3175	0.0000	1e-04		0.0000
Gsn	0.2827	0.0000	1e-04		0.0000
Ptgds	0.2822	0.0000	1e-04		0.0000
Ccl21a	0.2201	0.0000	1e-04		0.0000
Lcn2	0.1533	0.0000	1e-04		0.0000
Xcl1	0.1421	0.0000	1e-04		0.0000
Myl9	0.1347	0.0000	1e-04		0.0000
Tpm2	0.1255	0.0000	1e-04		0.0000
Col3a1	0.1060	0.0000	1e-04		0.0000
Vim	0.1056	0.0000	1e-04		0.0000
Ankrd23	0.1014	0.0000	1e-04		0.0000
Cfh	0.0980	0.0000	1e-04		0.0000
S100a8	0.0820	0.0000	1e-04		0.0000
Tent5c	0.0703	0.0000	1e-04		0.0000
S100a9	0.0609	0.0000	1e-04		0.0000
S100a4	0.0464	0.0000	1e-04		0.0000
Abca4	0.0327	0.0010	1e-04		0.0062
Hck	0.0308	0.0019	1e-04		0.0104
Stradb	0.0306	0.0020	1e-04		0.0104
Fubp1	0.0230	0.0147	1e-04		0.0733

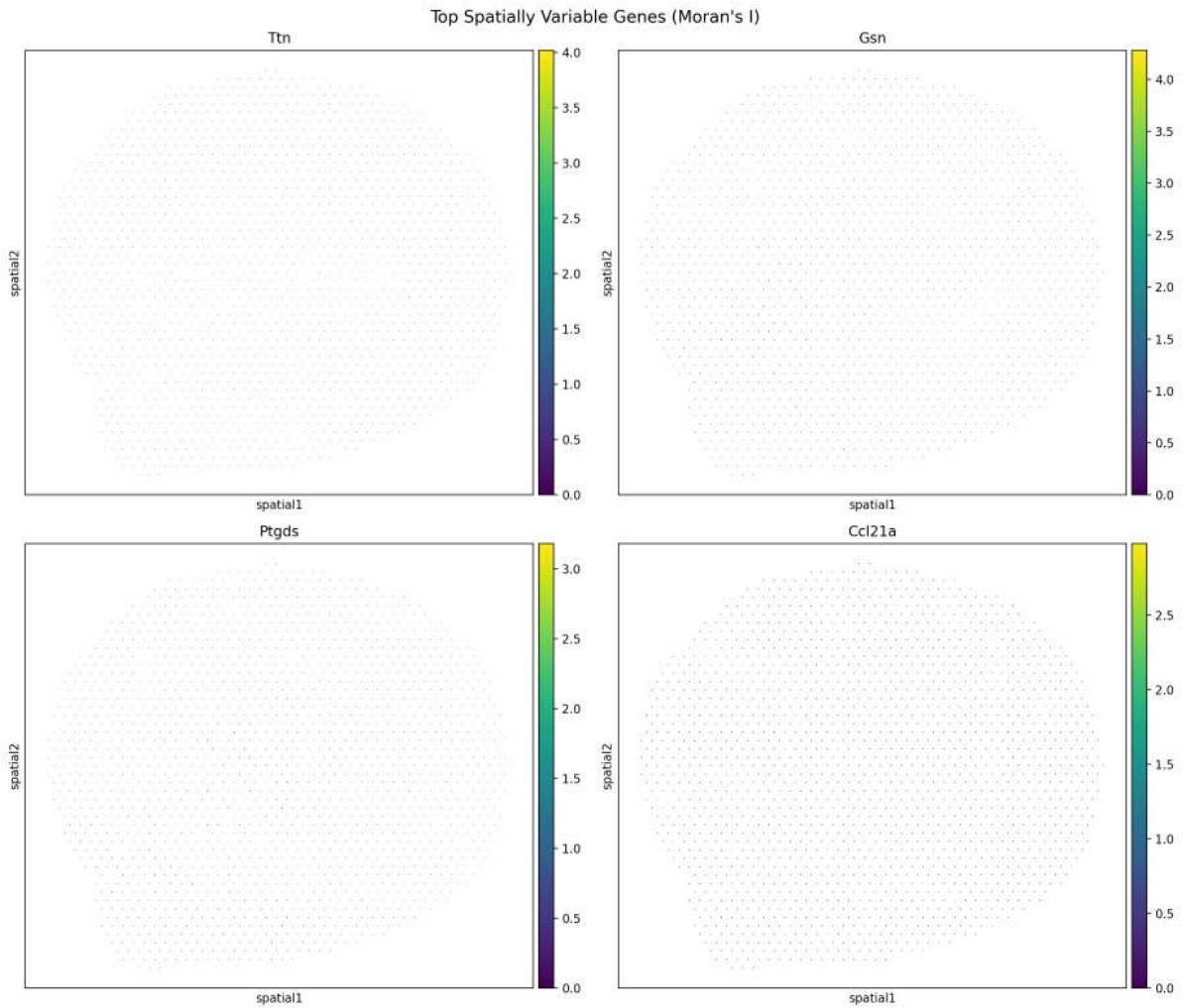


Figure 19: Top spatially variable genes colored by expression level.

## 9.2 Cell Type Spatial Mapping

Cell type labels were transferred from the scRNA-seq reference to spatial spots using marker gene scoring. Each spot was assigned the cell type with the highest enrichment score.

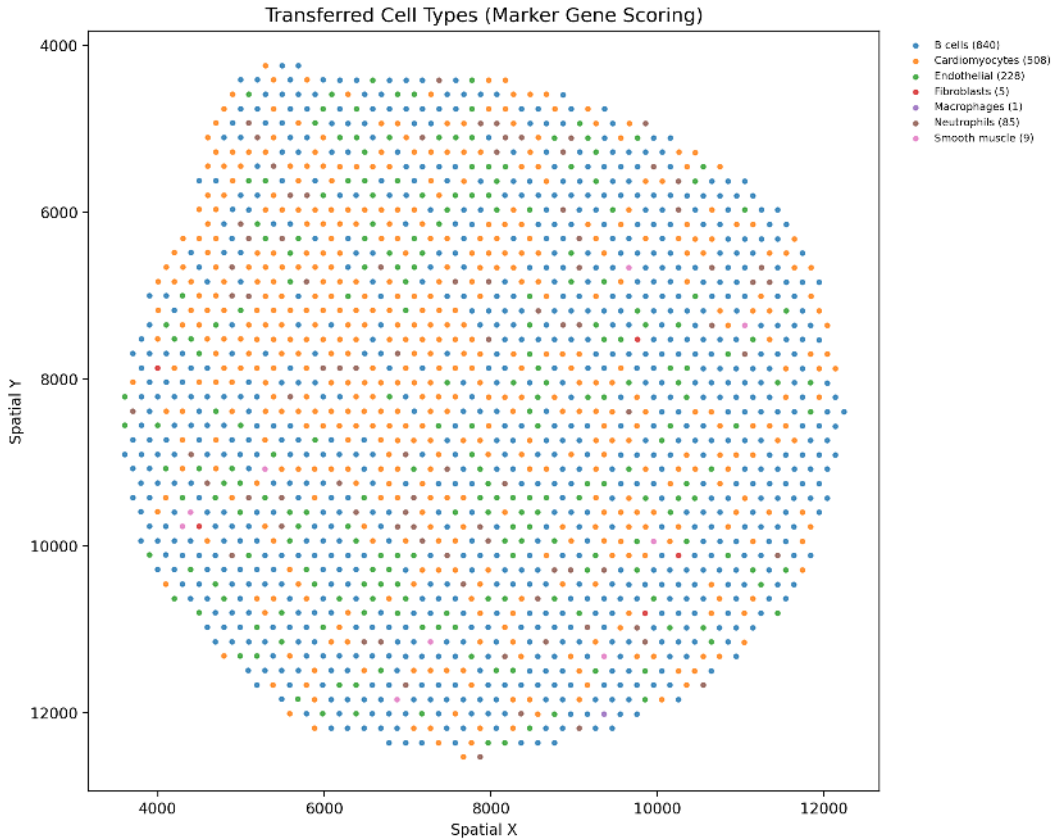


Figure 20: Spatial tissue map colored by transferred cell type labels from scRNA-seq reference.

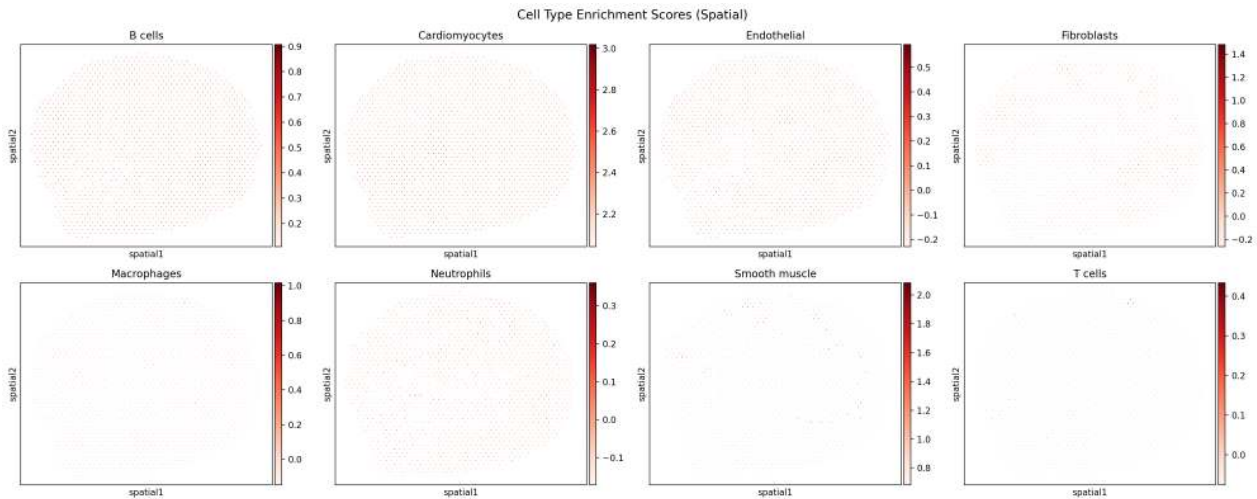


Figure 21: Per-cell-type enrichment scores across tissue. Darker red indicates higher marker gene set enrichment.

### 9.3 Differential Expression — Spatial Overlay

Top differentially expressed genes from the scRNA-seq condition comparisons are shown on the spatial tissue coordinates.

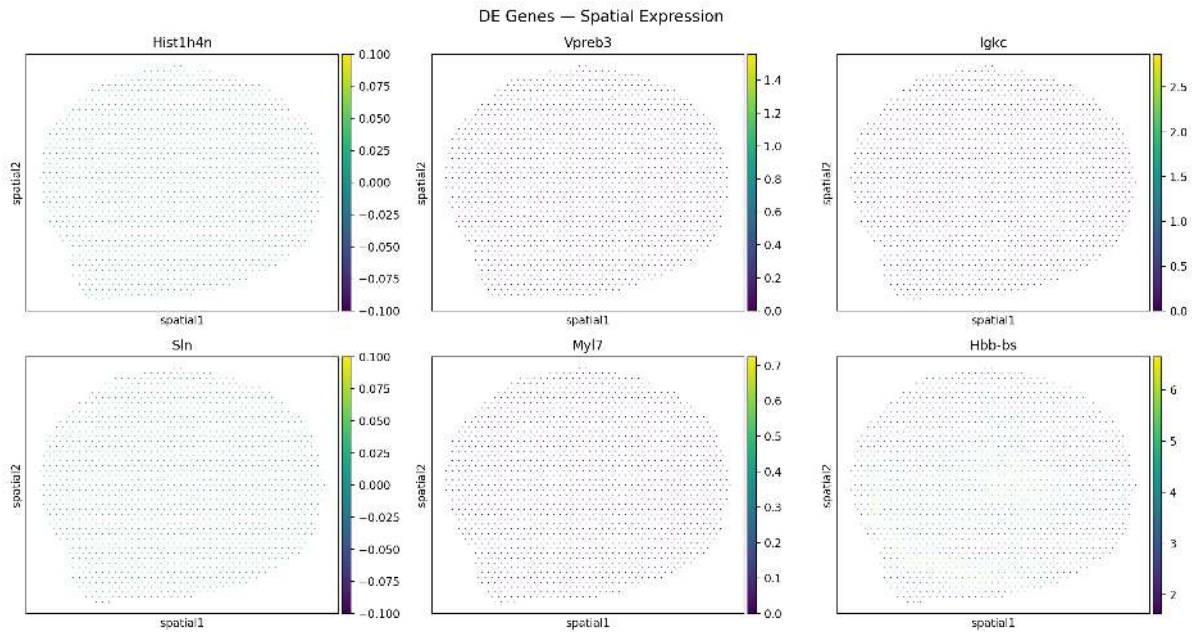


Figure 22: Spatial expression of top DE genes (scRNA-seq TAC vs Sham).

## 9.4 Cell Type Co-localization

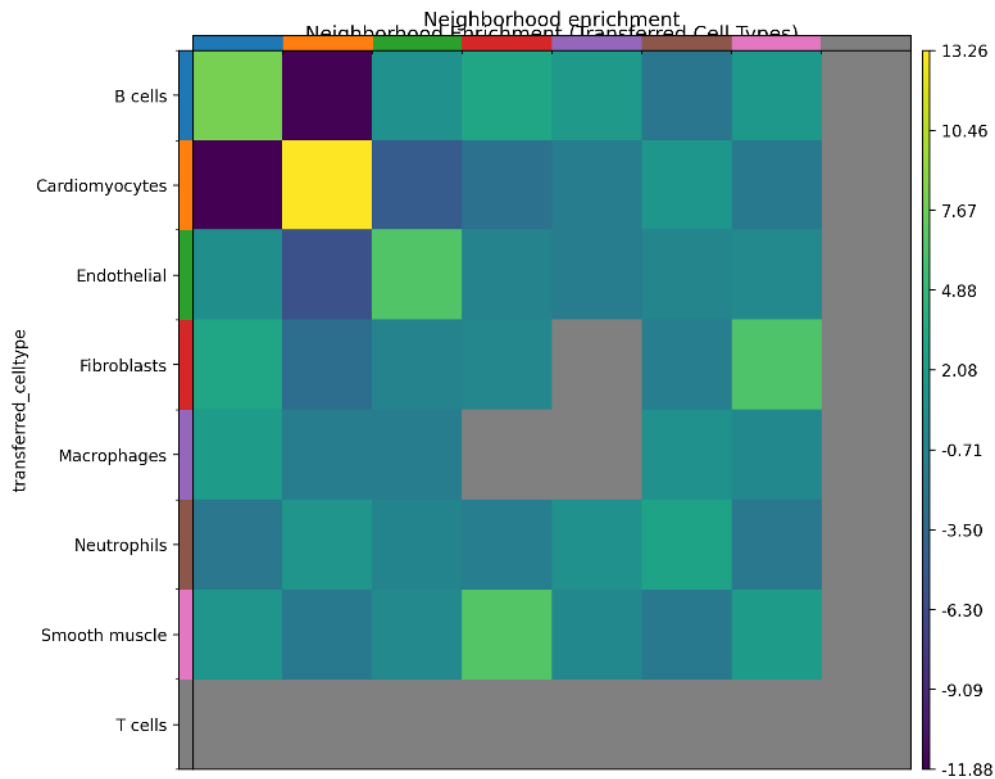


Figure 23: Neighborhood enrichment heatmap using transferred cell type labels. Positive values indicate spatial co-localization.

## 10 Conclusions

This single-cell analysis of the mouse TAC model reveals a clear spatiotemporal progression of myocardial remodeling at cellular resolution: 1. **Early response (2 weeks):** The transcriptomic signature is dominated by *Nppa* upregulation — the classical natriuretic peptide stress response — with minimal broader transcriptional changes. The cellular composition at this stage still resembles Sham, suggesting compensated hypertrophy. 2. **Late response (6 weeks):** A dramatic shift occurs, with 770 differentially expressed genes. Three key biological themes emerge: - **Immune infiltration:** B cell markers (*Igkc*, *Cd79a*) are among the most upregulated genes, and B cell proportions increase markedly in the composition data. This suggests an adaptive immune component to chronic heart failure that is often underappreciated in the TAC model literature. - **Mitochondrial dysfunction:** Five mitochondrial electron transport chain genes are significantly downregulated, consistent with the metabolic switch from fatty acid oxidation to glycolysis that characterizes the failing heart. - **Translational reprogramming:** Widespread upregulation of ribosomal proteins (*Rps/Rpl* family) suggests increased protein synthesis demands, possibly driven by the hypertrophic and fibrotic remodeling program. 3. **Clinical relevance:** The fibroblast-dominated microenvironment (41% of all cells) and its progressive shift toward immune-dominated composition mirrors findings in human heart failure biopsies, supporting the translational relevance of this model. These findings provide a cellular-resolution roadmap of heart failure progression and identify B cell infiltration and mitochondrial gene downregulation as potential therapeutic targets or biomarkers for disease staging.

---

*Report generated by GSE308859 Test Run project — 2026-04-03 16:58:37.485754 Pipeline: scanpy + Scrublet + Harmony + Leiden + CellTypist + Wilcoxon + scCODA + PAGA Deliverables: PDF report + Excel workbook (results\_workbook.xlsx) Full DEG tables available in the Excel workbook. For questions contact: alessandro.desantis@synmir.com*